



ACADEMIC  
PRESS

Available online at [www.sciencedirect.com](http://www.sciencedirect.com)

SCIENCE @ DIRECT®

NeuroImage

NeuroImage 19 (2003) 1449–1462

[www.elsevier.com/locate/ynimg](http://www.elsevier.com/locate/ynimg)

## Empirical analyses of null-hypothesis perfusion fMRI data at 1.5 and 4 T

Jiongjiong Wang,<sup>a,b,\*</sup> Geoffrey K. Aguirre,<sup>a,c</sup> Daniel Y. Kimberg,<sup>a</sup> and John A. Detre<sup>a,b</sup>

<sup>a</sup> Department of Neurology, University of Pennsylvania, 3400 Spruce St., Philadelphia, PA 19104, USA

<sup>b</sup> Department of Radiology, University of Pennsylvania, 3400 Spruce St., Philadelphia, PA 19104, USA

<sup>c</sup> Center of Cognitive Neuroscience, University of Pennsylvania, 3815 Walnut St., Philadelphia, PA 19104, USA

Received 16 August 2002; revised 13 February 2003; accepted 24 April 2003

### Abstract

Functional magnetic resonance imaging (fMRI) based on arterial spin labeling (ASL) perfusion contrast is an emergent methodology for visualizing brain function both at rest and during task performance. Because of the typical pairwise subtraction approach in generating perfusion images, ASL contrast manifests different noise properties and offers potential advantages for some experimental designs as compared with blood oxygenation-level-dependent (BOLD) contrast. We studied the noise properties and statistical power of ASL contrast, with a focus on temporal autocorrelation and spatial coherence, at both 1.5- and 4.0-T field strengths. Perfusion fMRI time series were found to be roughly independent in time, and voxelwise statistical analysis assuming independence of observations yielded false-positive rates compatible with theoretical values using appropriate analysis methods. Unlike BOLD fMRI data, perfusion data were not found to have spatial coherence that varied across temporal frequency. This finding has implications for the application of spatial smoothing to perfusion data. It was also found that the spatial coherence of the ASL data is greater at high magnetic field than low field, and including the global signal as a covariate in the general linear model improves the central tendency of test statistic as well as reduces the noise level in perfusion fMRI, especially at high magnetic field.

© 2003 Elsevier Inc. All rights reserved.

### Introduction

Arterial spin labeling (ASL) perfusion imaging is an emerging methodology for visualizing regional brain function both at rest and during activation (Detre and Alsop, 1999; Wong, 1999). This family of techniques use magnetically labeled arterial blood water as a diffusible tracer for quantitative measurement of cerebral blood flow (CBF) in a manner analogous to <sup>15</sup>O positron emission tomography (PET) scanning (Detre et al., 1994). Clinical applications have demonstrated the reliability of ASL techniques for CBF measurements in various cerebrovascular and psychiatric disorders (Detre and Wang, 2002). Although blood oxygenation-level-dependent (BOLD) contrast remains widely used for visualizing regional neural activation, ASL contrast is increasingly adopted for this purpose. Recent evidence suggests that ASL contrast might have certain advantages over BOLD contrast in functional magnetic

resonance imaging (fMRI) studies, including improved sensitivity at low task frequencies, reduced intersubject variability (Aguirre et al., 2002; Wang et al., 2003a), and more specific functional localization (Duong et al., 2001; Luh et al., 2000). In addition, perfusion contrast can be sampled using imaging sequences that preserve signal in brain regions of high static field inhomogeneity (Wang et al., 2003b), providing an alternative approach to optimized BOLD techniques with reduced sensitivity to macroscopic susceptibility effects (Cho et al., 1996; Constable and Spencer, 1999; Deichmann et al., 2002). In this article, we characterize and compare the noise properties and statistical power of ASL and BOLD techniques.

### Rationale and theory

#### *Independent observations in perfusion fMRI*

Functional MRI time series based on BOLD contrast possess temporal autocorrelation (Friston et al., 1994; Weiskoff et al., 1993), manifested as greater power in the lower

\* Corresponding author. Fax: +1-215-349-8260.

E-mail address: [jwang@rad.upenn.edu](mailto:jwang@rad.upenn.edu) (J. Wang).

frequency range of the power spectrum (Friston et al., 2000; Woolrich et al., 2001; Zarahn et al., 1997). With ASL methods, perfusion measurements are typically derived from pairwise subtractions of temporally adjacent images acquired with and without arterial spin labeling. Due to this pairwise subtraction, the slow (low-frequency) drifts present in BOLD contrast images are minimized in ASL data. It has been demonstrated in a recent study that ASL contrast has stable noise characteristics over the entire frequency spectrum and that perfusion data are statistically independent in time under the null hypothesis (Aguirre et al., 2002). This property of ASL has several significant implications for perfusion fMRI. First, ASL contrast is suitable for studying changes in neural activity that evolve over relatively long periods of time with reduced confounds from low-frequency noise. Correspondingly, sensorimotor activation, separated from the resting state as far as 1 day, has been successfully detected using ASL contrast (Wang et al., 2003a). Second, while “whitening” the BOLD data is very sensitive to bias (Friston et al., 2000; Woolrich et al., 2001), the inherent “white noise” property in ASL data simplifies statistical analysis and affords the opportunity to apply virtually any traditional parametric or nonparametric statistical test (Aguirre et al., 2002).

However, the validity of assuming independence of observations in the statistical analysis of perfusion fMRI data has not been systemically addressed. Although preliminary data suggested no substantial autocorrelation in perfusion data by averaging across-subject the voxel-based power spectrum, there remains the possibility of variations across subjects as well as across space within subject. For example, it may be the case that spatially discrete areas or tissue types evidence serial correlations in temporal noise, invalidating the standard general linear model (GLM) and inflating map-wise false-positive rates. The primary purpose of this study was to empirically test the hypothesis that perfusion data is independent in time by collecting perfusion fMRI time series in the absence of a temporally structured experimental paradigm (null-hypothesis data). A pulsed ASL (PASL) technique was used at both 1.5 and 4.0 T (Wang et al., 2002). In a manner similar to that applied to null-hypothesis BOLD fMRI data (Aguirre et al., 1997; Zarahn et al., 1997), periodic behavioral paradigms were assumed in the analysis and the observed false-positive rates for the test statistic using GLM were compared to the theoretical values.

#### *Spatially coherent noise*

Another important issue in fMRI analysis is the intrinsic spatial coherence of the voxel time series in fMRI noise data sets. Spatial coherence is akin to “smoothness” but also includes components of spatial correlation that cannot be captured by a continuously differentiable autocovariance function (e.g., measurements of full-width at half-maximum smoothness). Perhaps surprisingly, spatial coherence can be assessed (and vary) at different temporal frequencies — it is

in effect a measure of the degree to which power at a particular temporal frequency shares phase across space. In BOLD fMRI, spatial coherence has been found to vary systematically across temporal frequency in that lower temporal frequencies tend to share phase to a greater extent across space than high frequencies (Zarahn et al., 1997). As a consequence, spatial smoothing of BOLD data acts to augment temporal noise in the low-frequency range and can deleteriously impact experimental power (Aguirre et al., 1997).

Because it appears that perfusion fMRI data do not possess temporal autocorrelation in time under the null hypothesis, we might predict that there will not be an effect of temporal frequency on spatial coherence. On the other hand, physiological noise might introduce frequency-dependent spatial coherence into perfusion data, despite the absence of temporal correlation in the data in time. If present, such a pattern of spatial coherence would act to introduce temporal autocorrelation into perfusion fMRI data if it were smoothed in space. We therefore examined the spatial coherence of ASL data under the null hypothesis. A closely related measure is the global signal (the average of all brain voxel time series), the structure of which reflects spatial coherence. The global signal was assessed for different tissue types (gray and white matter and cerebrospinal fluid), and the effect of including the global signal as a covariate in the analysis of perfusion fMRI data was investigated.

#### *High- versus low-field ASL*

Although ASL perfusion fMRI provides some potential advantages compared to BOLD contrast, its widespread application in neuroimaging studies has been hampered by the relatively small signal change in functional activation, generally low temporal resolution, and the technical difficulty for implementation. Performing ASL fMRI at high magnetic field strength is appealing because it provides not only increased SNR but also advantages in terms of labeling effect due to the increased relaxation time T<sub>1</sub> of labeled blood. However, preliminary data comparing ASL techniques for functional activation studies at 1.5 and 4.0 T have not been encouraging. Although the ASL signal increases at high field, noise also increases, with no net improvement in sensitivity in motor cortex activation at 4.0 T as compared to ASL techniques at 1.5 T (Wang et al., 2002). If it were the case that spatially coherent noise (reflected as the global signal) was primarily responsible for this increase in noise at higher field strength, methods to remove the effects of global signal fluctuations might help to realize the SNR gain at high field. Therefore, assessments of spatial coherence and global signal were compared in ASL data acquired at both 1.5 and 4 T. To assess the impact of correction for global signal fluctuations at different field strengths, we also measured temporal noise before and after removal of global signal effects for these data sets.

In order to pursue the above three aims, the analyses of

the null-hypothesis data were accordingly structured into three primary sections: false-positive rate testing, spatial coherence measurement, and temporal fluctuation evaluation. Three documented subtraction approaches, namely “simple,” “surround,” and “sinc” subtraction (Aguirre et al., 2002; Wong et al., 1997), were employed to produce corresponding perfusion images along with a simultaneously derived BOLD data set for comparison. Both spatially unsmoothed and smoothed data sets were analyzed.

## Methods

### Imaging sequence

A modified version of the FAIR (Flow sensitive Alternating Inversion Recovery) (Kim, 1995) technique was used for perfusion fMRI, in which a saturation pulse was applied at  $TI_1 = 800$  ms after the global or slice-selective inversion, similar to QUIPSS II (Quantitative Imaging of Perfusion using a Single Subtraction) (Wong et al., 1998a). A slice-selective inversion pulse (FOCI “frequency offset corrected inversion,” 16 ms, BW 10k) (Ordidge et al., 1996) was used for arterial spin labeling, whereas the same pulse was used in the absence of gradients for global inversion during control labeling. The slab of the slice-selective inversion was 2 cm thicker than the imaging slab, leaving a pair of 1-cm margins at each edge of the imaging slices to ensure optimum inversion. The saturation pulse was applied to a 10-cm slab inferior to the imaging slices with a 1-cm gap between the adjacent edges of the saturation and imaging slabs. A delay time of 800 ms was applied between the saturation pulse and image acquisition to reduce transit related artifacts (Alsop and Detre, 1996). Interleaved tag and control images were acquired using a gradient-echo-echo-planar imaging (EPI) sequence, followed by a recovery time allowing the arterial blood to be refreshed.

### MR scanning

Imaging was performed on 1.5- and 4-T whole-body scanners (GE Medical Systems, Milwaukee, WI), with the standard product quadrature head coils. Except for the field strength and the use of an up/down converter to shift the resonant frequency, the 4-T scanner is identical in design to the 1.5-T scanner. Written informed consent was obtained prior to all human studies according to an Institutional Review Board approval. Perfusion imaging was performed on 10 healthy subjects (19–30 years, 5 female, mean 24.0 years) using the PASL sequence, the acquisition parameters were FOV =  $24 \times 16$  cm;  $64 \times 40$  matrix; TR/TE = 3000/18 ms; bandwidth, 100 kHz; slice thickness, 8 mm; interslice space, 2 mm. Eight slices were acquired from inferior to superior in an interleaved order to cover most of the brain cortex, and each slice acquisition took about 50 ms. Eight minutes of resting state perfusion scan (160 ac-

quisitions) was carried out on each subject using the PASL sequence at both field strengths. Subjects were instructed to relax with eyes open during the scan. “Dummy” gradient and RF pulses preceded the scan to allow tissue to reach steady-state magnetization. A 30-s two-point T1 measurement sequence was carried out after the scan for CBF quantification.

### Perfusion image generation

Perfusion image time series are generally produced by pairwise subtraction between interleaved label and control acquisitions. Several subtraction strategies have been proposed (Aguirre et al., 2002; Wong et al., 1997). The most straightforward approach, “simple subtraction,” uses direct pairwise subtraction between temporally adjacent label and control acquisitions. More complicated approaches use either linear (average of the two surrounding images) or sinc interpolation to shift the series of label (or control) images by one TR, followed by pairwise subtraction between time-matched label and control images. These methods are dubbed “surround subtraction” and “sinc subtraction” respectively. To investigate whether there is any difference between the noise properties of perfusion data generated using different subtraction approaches, all of these subtraction methods were assessed in data analyses. After the raw image series were reconstructed offline and motion corrected using a six-parameter, rigid-body, least-squares realignment routine (Friston et al., 1995), three separate difference perfusion image series were generated using the simple, surround, and sinc subtractions respectively. For comparison, one BOLD image series was obtained by taking the average of the time-matched label and control images produced using the sinc interpolation.

Absolute CBF ( $f$ ) image series were then calculated by (Wang et al., 2002) as follows;

$$f = \frac{\lambda \Delta M}{2\alpha M_0 T_{I_1} \exp(-T_{I_2}/T_{1a})} \quad (1)$$

where  $\Delta M$  is the difference perfusion image produced by the three subtraction methods respectively,  $M_0$  is the equilibrium brain tissue magnetization,  $\lambda$  is the blood/tissue water partition coefficient,  $T_{1a}$  is the longitudinal relaxation time of blood,  $\alpha$  is the inversion efficiency, and  $T_{I_2}$  is the time of image acquisition. Conversion to CBF values used assumed values of  $\lambda = 0.9$  ml/g (Raichle et al., 1976),  $\alpha = 0.98$  (Wong et al., 1998b),  $T_{1a} = 1.2$  s at 1.5 T and 1.6 s at 4.0 T (Bottomley et al., 1987), and the  $M_0$  image acquired with the T1 measurement sequence. To minimize the motion artifact between the  $M_0$  and functional images, the  $M_0$  images were also realigned to the precedent functional scan by applying the transformation matrix of the last image of that scan.

### Spatial smoothing

The three CBF image series and one BOLD image series derived from the 8-min scan at each field strength were smoothed using a three-dimensional 11-mm full-width at half-maximum (FWHM) Gaussian kernel. The size of this kernel is typical for functional neuroimaging studies.

### False-positive rate comparisons

Eight noise image series obtained at each field strength were analyzed using the VoxBo software package (<http://www.voxbo.org>), i.e., six series of unsmoothed and smoothed CBF images generated using the simple, surround, and sinc subtractions respectively, and two series of unsmoothed and smoothed BOLD images. A GLM with assumption of independent observations was applied to each noise image series to empirically determine the false-positive rates for assumed behavioral paradigm effects. Two pseudobehavioral paradigms were assumed with relatively high (0.0167 Hz, 30 s OFF/ON) and low (0.0021 Hz, 4 min OFF/ON) fundamental frequencies, representing a spectrum of experimental designs that may be exploited in perfusion fMRI (Wang et al., 2003a). GLM versions with or without inclusion of the global signal as a covariate were applied, and  $t$  testing was used to evaluate the significance of the variance in the data explained by the model.

False-positive rates were characterized by the percentage of voxels in each image series with  $t$  values (absolute value) greater than the two-tailed nominal  $\alpha = 0.05$  threshold, hereafter referred to as FP1. This is a gross measure of the width of the noise distributions, and the theoretically expected value of FP1 was 5% in both unsmoothed and smoothed data sets. False-positive rates were also measured by the proportion of data sets that contained at least one voxel with a  $t$  value (absolute value) greater than the two-tailed nominal  $\alpha = 0.05$  threshold that has been corrected for multiple comparison, hereafter referred to as FP2. Two methods were used for the correction of multiple comparisons: Gaussian random field theory which takes into account the spatial smoothness of the data (Worsley et al., 1996, 2002) and a simple Bonferroni correction based on the number of voxels in the brain. The final threshold is the minimum of the two. The theoretically expected value of FP2 was also 5%. The hypothesis that the central tendency of FP1 was different from 5% was tested with the unpaired  $t$  test (two-tailed), and the hypothesis that FP2 was greater than 5% was tested with the binomial distribution (one-tailed) for both spatially smoothed and unsmoothed data using the two assumed behavioral paradigms respectively (nonparametric methods like signed rank test gave identical results). In addition, the measurements of FP1 were entered into repeated-measures ANOVA using the SPSS software package for the BOLD and perfusion data respectively, to assess effects of spatial smoothing (with or without), field strength (1.5 or 4.0 T), task frequency (high or low), and

subtraction methods (simple, surround, or sinc for perfusion data only).

### Estimation of smoothness and spatial coherence

The smoothness and spatial coherence of the noise data were measured using three methods, respectively. In the first approach, the spatial coherence (SC) as a function of temporal frequency was determined for each data set according to (Zarahn et al., 1997)

$$SC(\omega) = \frac{\left[ \frac{PS_{\text{global signal}}(\omega)V}{PS_{\text{voxel averaged}}(\omega)} \right] - 1}{V - 1}, \quad (2)$$

where  $PS_{\text{global signal}}(\omega)$  is the power spectrum of the global signal at temporal frequency  $\omega$ ,  $PS_{\text{voxel averaged}}(\omega)$  is the voxel-averaged power spectrum at temporal frequency  $\omega$ , and  $V$  is the voxel count for the data set.  $SC(\omega)$  is expected to vary from 0 to 1 as the cross-correlation between voxels at temporal frequency  $\omega$  varies from 0 to 1.

The second approach measures the spatial characteristic of the global signal by correlating each voxel time series with the global signal (average of all voxel time series) to create correlation coefficient maps. These maps represent the spatial distribution of the relative presence of the global signals throughout the volumetric data sets. According to the T1 images calculated from the T1 measurement sequence, three region-of-interest (ROI) of gray matter, white matter, and cerebrospinal fluid (CSF) were identified based on the particular T1 range associated with each type of tissue at 1.5 and 4.0 T, respectively (Bottomley et al., 1987). The global mean correlation coefficient averaged across all the brain voxels and the mean correlation coefficients averaged across the voxels within the ROIs of gray matter, white matter, and CSF were obtained in each data set. The correlation measurements were analyzed using repeated-measures ANOVA for the BOLD and perfusion data respectively, with analysis factors of spatial smoothing, field strength, and tissue type.

In the third approach, the smoothness of the statistical maps was assessed using the residuals of the GLM, as described by (Kiebel et al., 1999). This measure yields the FWHM of a Gaussian kernel that would have to be applied to a volume of spatially independent noise to achieve an equivalent degree of smoothness. The three measurements of spatial coherence and map smoothness described above focus on different aspects of the spatially coherent noise and may produce different results. The spatial coherence measurement and correlation analysis probe the temporal and spatial characteristics of the spatially coherent noise respectively, whereas the voxel size of FWHM provides a single measure of map smoothness at a particular task frequency and is dependent on the choice of GLM. Note the conceptual difference between “spatial coherence” and “spatial frequencies,” which can only be ascertained using transfor-

mation-based techniques such as spatial wavelet and LaPlace deconvolution.

### Temporal fluctuation

The temporal fluctuation level in each image series was characterized by voxelwise normalized temporal standard deviation (SD), determined by the temporal SD divided by the  $M_0$  signal in each voxel. The raw difference perfusion image series ( $\Delta M$ ) were analyzed to generate a measure of temporal fluctuation as fractional variation in  $M_0$ , which could be compared to the corresponding measure in BOLD data. Both the histogram of the normalized SD and the global mean normalized temporal SD averaged across all the brain voxels were obtained. To assess the effect of the spatially coherent noise, new image series were generated by removing the spatially coherent noise from the original data through orthogonalizing the voxel time series with the mean normalized global signal (with zero mean). This procedure is similar to using the global signal as a single covariate in the GLM analysis and obtaining the residual time series that cannot be explained by the global signal. These new image series were then subject to the measurement of normalized temporal SD as mentioned above. All the temporal fluctuation results were entered into repeated-measures ANOVA for the BOLD and perfusion data, respectively, to assess effects of spatial smoothing, field strength, orthogonalization with the global signal, and subtraction methods (for perfusion data only).

## Results

### Empirical appearance of power spectra

Figure 1 displays the mean power spectra averaged across space and subjects, using either unsmoothed or smoothed noise data at each field strength respectively. Compared to the spectra of the BOLD data that evidence greatly increased power at low temporal frequencies, the perfusion data generated by the three subtraction approaches all show relatively stable noise characteristics over the whole frequency spectrum. However, small deviations from the strictly even distribution of power spectra do exist. For example, both the unsmoothed and smoothed perfusion data at 1.5 and 4.0 T produced using surround subtraction manifest a trend of progressively increased power with ever lower temporal frequency (red lines), although the trend is fairly small compared to BOLD data. The unsmoothed perfusion data at both field strengths generated with simple subtraction has higher power at the lowest temporal frequency. However, this phenomenon is absent in the smoothed simple subtraction perfusion data. The sources and effects of these deviations from the rigorously even distribution of the power spectrum in perfusion data are examined and discussed in the following sections.

### Examination of false-positive rates

The values of the mean percentage FP1 averaged across 10 subjects and the mapwise FP2 are tabulated in Tables 1a and 1b for the spatially unsmoothed and smoothed data, respectively. In all the analyses described in this section, the global signal is included as a covariate since this approach would improve the central tendency of the distribution of test statistic to 0 while keeping the mean and variance of false-positive rate results unchanged, as is demonstrated below. For BOLD data, the false-positive rates are slightly greater than but not significantly different from theoretically expected when the behavioral paradigm of 30 s OFF/ON is assumed. In contrast, the false-positive rates are far in excess of what would be expected using the assumed paradigm of 4 min OFF/ON with more than half of the voxels displaying pseudoactivation, resulting in significant main effect of task frequency [ $F(1, 9) = 260.5, P < 0.001$ ]. This observation again confirms the substantial autocorrelation in BOLD time series and the limitation of BOLD contrast in studying slow changes in neural activity because of the confounding effect from low-frequency noise (Aguirre et al., 2002; Friston et al., 2000). It is also interesting that the percentage of voxels (FP1) exceeding the  $\alpha = 0.05$  threshold is increased in the smoothed BOLD data compared with the unsmoothed data, resulting in significant main effect of spatial smoothing [ $F(1, 9) = 44.0, P < 0.001$ ]. A significant spatial smoothing  $\times$  task frequency interaction is observed [ $F(1, 9) = 23.6, P = 0.001$ ], indicating the effect of smoothing is stronger at low task frequency than high frequency for the BOLD data. This phenomenon is explained by the previous observation that the spatial coherence in BOLD data is greater at lower temporal frequencies (Zarahn et al., 1997). No significant main effect of field strength is found.

For perfusion data, both the unsmoothed and smoothed data have similar levels of false-positive rates, and the measurements from the smoothed data show improvements to be slightly more consistent with the tabular value compared to the unsmoothed data. The simple subtraction provides false-positive rates well matching the theoretically expected value with all the FP1s and FP2s measured at both field strengths using two assumed paradigms consistent with the 5% threshold. The sinc subtraction data also show good agreement with the tabular value, with one FP1 measured at 4 T using high task frequency being slightly lower than the 5% threshold. The surround subtraction approach, however, yields excessive false-positive rates especially for the low task frequency. All FP1s and 2 FP2s measured using low task frequency surpass the theoretically expected value, although this effect is not statistically significant for two FP1 measures in the smoothed surround subtraction data. The result of excessive false-positive rates in perfusion data generated using the surround subtraction is in agreement with the observed small trend of greater power at lower temporal frequency in the corresponding power spectrum.

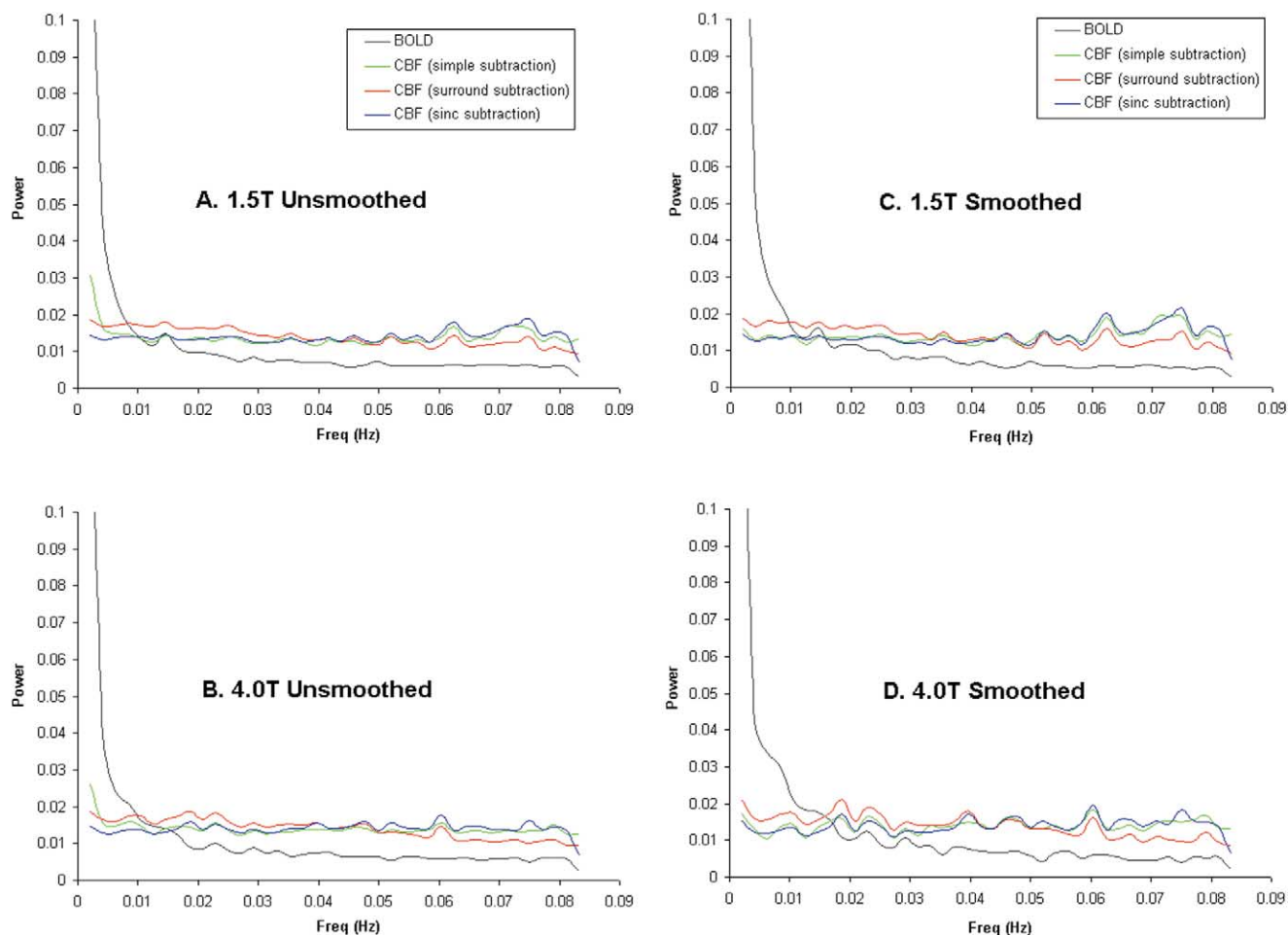


Fig. 1. The mean power spectra averaged across space and subjects, using either spatially unsmoothed (A and B) or smoothed (C and D) data sets at 1.5 T (A and C) and 4.0 T (B and D). Spectra of perfusion data sets generated using simple, surround, and sinc subtractions and one concurrently derived BOLD data set are shown. In contrast to the perfusion data, BOLD data show markedly increased power at low frequencies. The surround subtraction perfusion data shows a small trend of increased power at lower frequencies.

The above results are further confirmed by the repeated-measures ANOVA analysis on the measures of FP1 that show significant main effect of subtraction method [ $F(2, 8) = 426.0, P < 0.001$ ] along with a significant task frequency  $\times$  subtraction method interaction [ $F(2, 8) = 12.5, P = 0.003$ ], which could be attributed to the greater FP1 measures at low task frequency as compared to those at high frequency in the surround subtraction data. The results also show a significant smoothing  $\times$  subtraction method interaction [ $F(2, 8) = 4.8, P = 0.043$ ], probably reflecting the more prominent improvement in FP1 measures of the sur-

round subtraction perfusion data after spatial smoothing. No significant effect for spatial smoothing, field strength, or task frequency is observed.

#### Measurement of map smoothness and spatial coherence

For simplicity, the measurements of map smoothness and spatial coherence derived using the sinc subtraction are presented in this section and compared to the BOLD data, because all the three subtraction methods yield very similar results. The results of the SC measurement on the un-

Fig. 3. The correlation maps of a representative subject based on perfusion data acquired at 1.5 and 4.0 T, generated by correlating each voxel time series with the global signal. The perfusion data presented here is produced by the sinc subtraction approach, and color scale of correlation coefficients are superimposed upon the mean CBF images generated by averaging the perfusion image series. The top two panels display correlation maps of unsmoothed perfusion data at 1.5 and 4.0 T respectively, and threshold of correlation coefficient is arbitrarily set as 0.25. The bottom two panels display correlation maps of smoothed perfusion data at 1.5 and 4.0 T respectively, and threshold is arbitrarily set as 0.5.

Fig. 4. The histogram of voxel-based measures of normalized temporal SD in the smoothed perfusion data acquired at 1.5 and 4.0 T before and after removing the spatially coherent noise. The histogram is averaged across individual data sets and the perfusion data are generated using sinc subtraction. Removing the global signal from each voxel time series by orthogonalization improves temporal fluctuation of the smoothed 4.0-T data much more than the 1.5-T data.

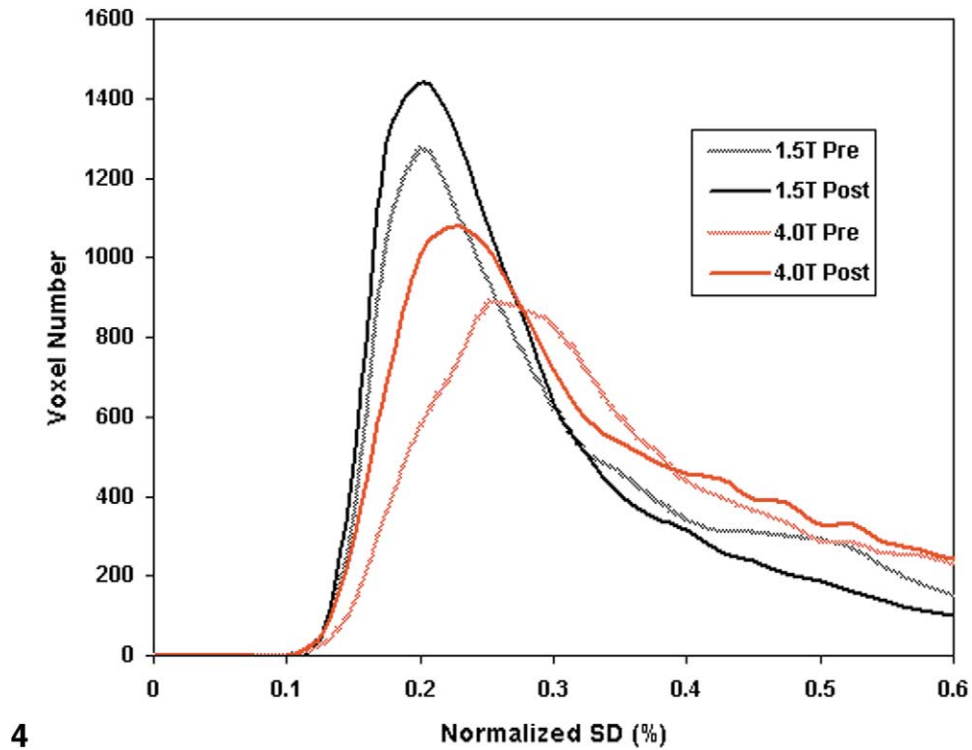
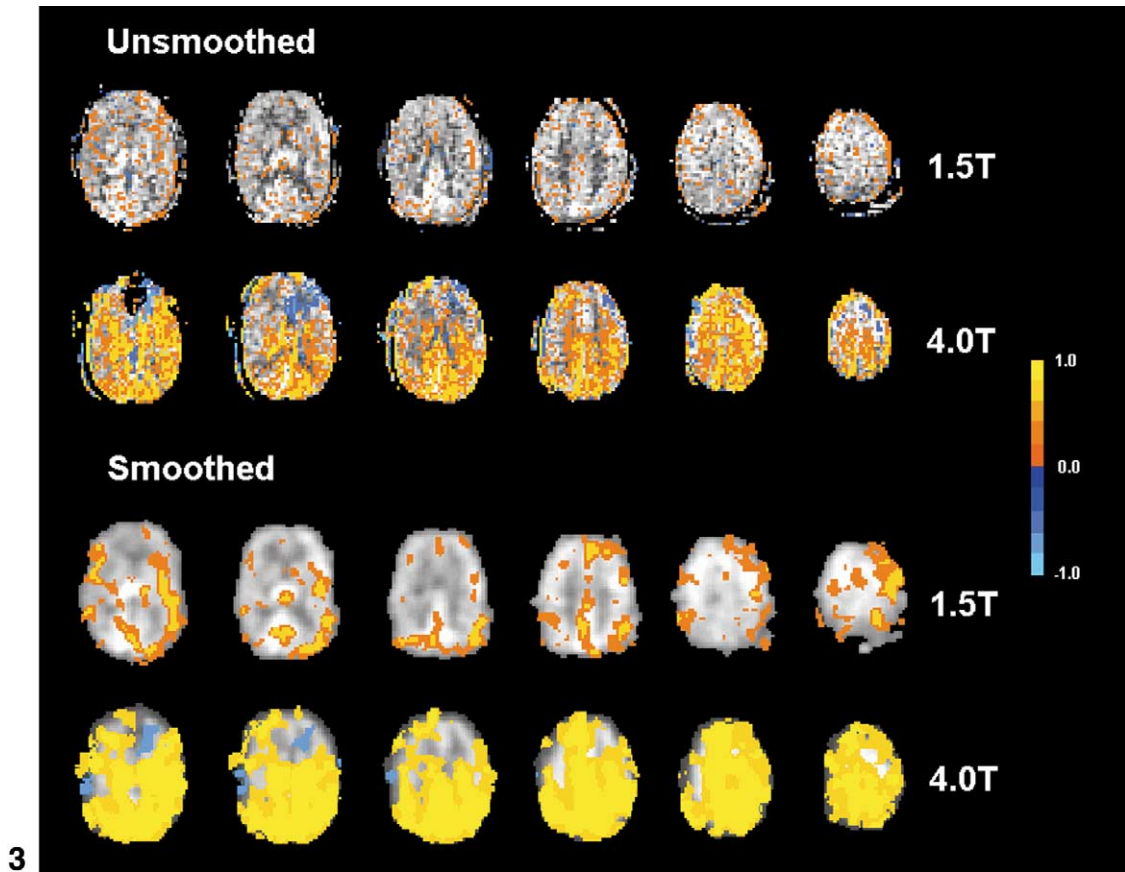


Table 1a  
Voxel-based and mapwise false-positive rates (FP1 and FP2 respectively) measured in the unsmoothed perfusion and BOLD data

	High task frequency		Low task frequency	
	1.5 T	4.0 T	1.5 T	4.0 T
<b>FP1</b>				
BOLD	0.058	0.057	0.504*	0.600*
ASL (simple subtraction)	0.048	0.044	0.050	0.048
ASL (surround subtraction)	0.069*	0.069*	0.086*	0.087*
ASL (sinc subtraction)	0.046	0.042*	0.050	0.051
<b>FP2</b>				
BOLD	0/10	1/10	10/10 <sup>†</sup>	10/10 <sup>†</sup>
ASL (simple subtraction)	0/10	0/10	1/10	1/10
ASL (surround subtraction)	0/10	1/10	4/10 <sup>†</sup>	4/10 <sup>†</sup>
ASL (sinc subtraction)	0/10	0/10	2/10	1/10

Note. FP1s are averaged across 10 subjects.

\* Indicates FP1 significantly different from 5% threshold ( $P < 0.05$ , two-tailed unpaired  $t$  test).

<sup>†</sup> Indicates FP2 significantly different from 5% threshold ( $P < 0.05$ , one-tailed binomial distribution test).

smoothed data as a function of temporal frequency are shown in Fig. 2. In all the data sets tested, the SC measure is greater than 0 across the whole frequency range, showing spatial coherence existing at all frequencies in both BOLD and perfusion data. The SC of the BOLD data is greater at low frequencies compared to high at both 1.5 and 4.0 T, consistent with previous findings (Zarahn et al., 1997). By contrast, the SC measure in perfusion data is relatively consistent across frequencies. This difference in the temporal characteristics of the SC measures in BOLD and perfusion data explains our observation that spatial smoothing increases the false-positive rate for BOLD data.

The spatial characteristics of the global signal in both perfusion and BOLD data are measured by correlating each voxel time series with the global signal to create correlation coefficient maps. The mean correlation coefficients averaged across the whole brain, ROIs of gray matter, white matter, and CSF are tabulated in Table 2, and the results from the sinc subtraction perfusion data are used as the representative of ASL data due to the resemblance of the results from three subtraction methods. All the data sets have positive correlations with the global signal, indicating spatial coherence is an intrinsic property with both perfusion and BOLD data. Not surprisingly, spatially smoothed data have greatly increased correlation coefficients compared with unsmoothed data, manifested as significant main effect of spatial smoothing [ $F(1, 9) = 575.9.4$  for perfusion;  $F = 415.3$  for BOLD,  $P < 0.001$ ]. Figure 3 displays the correlation maps of the global signal of a representative subject based on perfusion data acquired at 1.5 and 4.0 T. As obviously shown in Fig. 3, 4.0-T data have greater

spatial coherence than 1.5-T data, and the difference is statistically significant [ $F(1, 9) = 37.6$  for perfusion;  $F = 34.9$  for BOLD,  $P < 0.001$ ]. The mean CBF images are overlaid which show global perfusion (averaged across 10 subjects) of  $69.3 \pm 6.7$  and  $59.1 \pm 10.8$  ml/100 g/min at 1.5 and 4 T, respectively. The CBF values match well with our previous results (Wang et al., 2002) as well as other ASL studies (Alsop and Detre, 1996; Yang et al., 1998; Ye et al., 1997). No significant difference is found between the ROI-based measurements of gray matter, white matter, and CSF at both 1.5 and 4.0 T in the perfusion and BOLD data, consistent with previous finding that global signal in BOLD data does not segregate strongly to certain type of neuro-anatomic tissue (Zarahn et al., 1997). Statistical analyses also demonstrate that the global signal correlation is significantly higher in the BOLD data compared to perfusion data [ $F(1, 9) = 206.8$ ,  $P < 0.001$ ], which might imply that the noise in perfusion image series is less spatially coherent than in BOLD data.

Table 3 lists the estimated map smoothness as the voxel size of FWHM at 1.5 and 4.0 T with both the low- and high-frequency paradigms respectively. Again sinc subtraction data are used as the representative of the perfusion data. Global signal is included as a covariate in the analysis; excluding the global signal as a covariate yields increased FWHM measures in both BOLD and perfusion data but does not affect the results reported below. In general, there is a trend of larger size of FWHM at 4.0 T than at 1.5 T that supports the results from the correlation analysis [ $F(1, 9) = 5.4$ ,  $P = 0.046$  for BOLD;  $F = 9.9$ ,  $P = 0.012$  for perfusion]. Not surprisingly, larger FWHM in the spatially

Table 1b  
Voxel-based and mapwise false-positive rates (FP1 and FP2 respectively) measured in the smoothed perfusion and BOLD data

	High task frequency		Low task frequency	
	1.5 T	4 T	1.5 T	4 T
<b>FP1</b>				
BOLD	0.065	0.061	0.584*	0.640*
ASL (simple subtraction)	0.044	0.041	0.053	0.049
ASL (surround subtraction)	0.063*	0.064	0.088*	0.083
ASL (sinc subtraction)	0.042	0.037*	0.054	0.054
<b>FP2</b>				
BOLD	0/10	1/10	10/10 <sup>†</sup>	10/10 <sup>†</sup>
ASL (simple subtraction)	0/10	0/10	0/10	0/10
ASL (surround subtraction)	0/10	0/10	4/10 <sup>†</sup>	3/10 <sup>†</sup>
ASL (sinc subtraction)	0/10	0/10	0/10	0/10

Note. FP1s are averaged across 10 subjects.

\* Indicates FP1 significantly different from 5% threshold ( $P < 0.05$ , two-tailed unpaired  $t$  test).

<sup>†</sup> Indicates FP2 significantly different from 5% threshold ( $P < 0.05$ , one-tailed binomial distribution test).

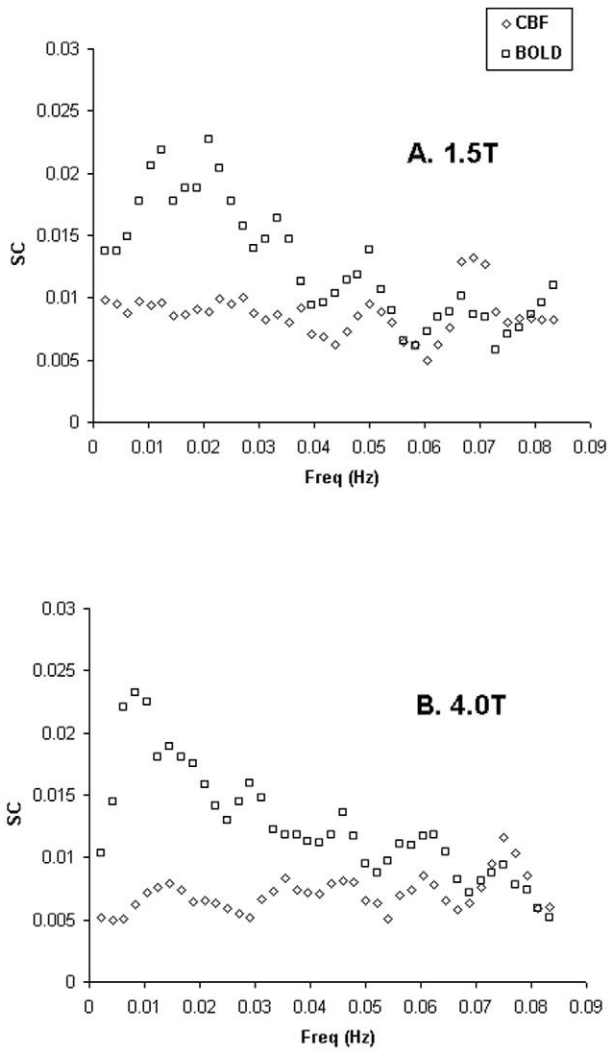


Fig. 2. The mean spatial coherence as a function of temporal frequency averaged across space and subjects. The SC measurements from spatially unsmoothed sinc subtraction data acquired at 1.5 T (A) and 4.0 T (B) are shown. Note the difference of the SC measures in perfusion and BOLD data at low frequency range in both images.

smoothed data is observed as compared to unsmoothed data [ $F(1, 9) = 1122.2$  for BOLD;  $F = 737.5$  for perfusion,  $P < 0.001$ ]. Interestingly, the FWHM measures are smaller at low task frequency compared to high frequency in the BOLD data, resulting in a significant main effect of task frequency [ $F(1, 9) = 91.9$ ,  $P < 0.001$ ]. A significant interaction of spatial smoothing and task frequency is also observed in BOLD data [ $F(1, 9) = 38.0$ ,  $P < 0.001$ ], suggesting smoothing enhances the map smoothness more at high versus low task frequency. Statistical analyses also demonstrate the map smoothness is significantly lower in the BOLD data compared to perfusion data [ $F(1, 9) = 46.2$ ,  $P < 0.001$ ]. This seemingly contradictory result—given the finding of the correlation analysis above—probably arises because map smoothness is derived from the residuals of the general linear model (Kiebel et al., 1999). Spatially coherent noise is more likely to be explained by the assumed behav-

Table 2

Mean correlation coefficient with global signal as the reference function

	Unsmoothed		Smoothed	
	1.5T	4T	1.5T	4T
Global				
BOLD	0.206	0.386	0.465	0.627
ASL	0.120	0.252	0.332	0.514
Gray matter				
BOLD	0.212	0.393	0.454	0.621
ASL	0.115	0.257	0.336	0.518
White matter				
BOLD	0.230	0.373	0.555	0.651
ASL	0.095	0.259	0.308	0.534
CSF				
BOLD	0.175	0.366	0.404	0.606
ASL	0.153	0.220	0.334	0.467

ior paradigm in the BOLD data compared to perfusion data. On similar account, the FWHM measures are smaller at low task frequency in the BOLD data, since the spatial coherence of the BOLD time series is easier explained by an assumed function of low frequency than high frequency.

The above measures of the map smoothness and spatial coherence show that the global signal in both BOLD and perfusion fMRI image series is a spatially coherent process, and this effect of spatial coherence seems to increase with field strength (at least using the current ASL technique). As previously shown, the inclusion of the global signal improves the center tendency of the distribution of  $t$  statistic to be close to 0 in the BOLD data (Zarahn et al., 1997). Similar effects are observed in the perfusion data as the  $t$  distribution of the perfusion data is much less biased when the global signal is included as a covariate in the GLM analysis. The difference between the number of voxels exceeding the  $\alpha = 0.05$  threshold in the positive and negative tails is found to be significantly lower when the global signal is included than when the global signal is excluded [ $F(1, 9) = 11.5$ ,  $P = 0.008$ ]. No effect of global signal is observed on the mean and variance of the false-positive rate measures.

Evaluation of temporal fluctuation

The measures of voxel-based temporal fluctuation with respect to  $M_0$ , defined as the normalized temporal SD of the

Table 3

Mean map smoothness measured as voxel size of FWHM

	High task frequency		Low task frequency	
	1.5 T	4 T	1.5 T	4 T
FWHM (unsmoothed)				
BOLD	1.344	1.389	1.336	1.374
ASL	1.360	1.398	1.360	1.398
FWHM (smoothed)				
BOLD	2.439	2.561	2.381	2.513
ASL	2.787	3.071	2.772	3.071

Table 4  
Mean voxel-based temporal fluctuation pre- and postorthogonalization with the global signal

	Unsmoothed		Smoothed	
	1.5T	4T	1.5T	4T
Preorthogonalization with global signal				
BOLD	0.0079	0.0105	0.0051	0.0077
ASL (simple subtraction)	0.0102	0.0127	0.0038	0.0065
ASL (surround subtraction)	0.0093	0.0112	0.0033	0.0052
ASL (sinc subtraction)	0.0101	0.0124	0.0038	0.0060
Postorthogonalization with global signal				
BOLD	0.0074	0.0086	0.0044	0.0051
ASL (simple subtraction)	0.0099	0.0116	0.0034	0.0045
ASL (surround subtraction)	0.0090	0.0104	0.0029	0.0038
ASL (sinc subtraction)	0.0099	0.0115	0.0033	0.0044

voxel time series, are listed in Table 4. The mean normalized temporal SD of the perfusion and BOLD data are comparable, with no significant difference between the two measures.

Interestingly, the temporal fluctuation of the perfusion time series is larger than that of BOLD in unsmoothed data while the trend is reversed in spatially smoothed data, resulting in a highly significant interaction of smoothing and imaging contrast [ $F(1, 9) = 150.1, P < 0.001$ ]. It suggests that spatial smoothing is more beneficial in reducing the temporal noise in perfusion than BOLD data, probably due to the strengthened drift effects in smoothed BOLD data. The temporal SD values measured in 4.0-T perfusion data are larger compared to those at 1.5 T [ $F(1, 9) = 4.9, P = 0.053$ ], primarily due to the increased noise level at 4.0 T even though the ASL signal is also increased (Wang et al., 2002). This difference becomes more pronounced in the spatially smoothed data because the noise of high field image series is more spatially coherent than at low field, as demonstrated above. As expected, spatial smoothing significantly reduces the noise level in both BOLD and perfusion data [ $F(1, 9) = 508.1$  for perfusion;  $F = 2811$  for BOLD,  $P < 0.001$ ].

The measures of voxel-based temporal fluctuation in new image series, generated by removing spatially coherent noise from the original data through orthogonalizing the voxel time series with the global signal (as a single covariate in GLM), are also listed in Table 4. Removing the spatially coherent noise is found to reduce the temporal fluctuation in both perfusion and BOLD image series, and the main effect of orthogonalization with global signal is significant for perfusion data [ $F(1, 9) = 6.3, P = 0.034$ ] but displays a trend for BOLD data [ $F(1, 9) = 4.4, P = 0.064$ ]. The effect of orthogonalization with global signal is more prominent at 4.0 T compared to 1.5 T in the perfusion data, resulting in a (nearly) significant interaction of orthogonalization and field strength [ $F(1, 9) = 5.0, P = 0.052$ ]. Figure 4 demonstrates the effect of removing spatially coherent

noise on the histogram of the voxel-based normalized SD of the smoothed perfusion data, the distribution of normalized SD at 4.0 T displays more prominent improvement compared to that at 1.5 T after the global signal is removed from each voxel time series. A similar effect is present in the BOLD data (not shown), but at a less prominent level which does not reach statistical significance. These results suggest that spatial smoothing plus inclusion of the global signal as a covariate in the GLM could improve the functional sensitivity of perfusion fMRI, especially at high field.

Another observation from the above analyses is that the noise level in the perfusion data generated using the three subtraction methods is lowest in the surround subtraction data, manifested as significant main effect of subtraction methods [ $F(2, 8) = 101.8, P < 0.001$ ]. This phenomenon is actually related to the different effects of the three methods in producing the false-positive rates in each corresponding data set, as is discussed below. The 4.0-T BOLD data have significantly increased noise level compared to 1.5-T BOLD data [ $F(1, 9) = 6.1, P = 0.035$ ], which seems to contradict previous data showing improved sensitivity at 4.0 T for BOLD contrast (Yang et al., 1999). However, the current results are based on imaging parameters optimized for perfusion imaging that might impose different effects on the concurrently acquired BOLD data compared to optimized BOLD imaging, as is also discussed below.

## Discussions

The present study demonstrated that the ASL perfusion fMRI time series acquired in null-hypothesis conditions do not have substantial temporal autocorrelation at either 1.5 or 4.0 T. Therefore, statistical analyses of perfusion fMRI data that assume independence of observations are valid. The stable statistic of the perfusion fMRI data with assumed behavioral paradigms of both low and high task frequencies suggest a wider range of experimental designs may be feasible for perfusion fMRI covering time scales of seconds, minutes, hours, and even days (Wang et al., 2003a). In particular, perfusion fMRI is suitable for studies of slowly developing processes (e.g., mood changes or procedural learning) as well as studies that require comparison of widely-spaced observations (e.g., drug effects). By contrast, BOLD fMRI provides increased sensitivity for relatively high frequencies of experimental design, especially event-related designs that prevail in functional neuroimaging studies.

The mechanism of low-frequency noise in BOLD fMRI data is still unclear. Drift effects have been shown to be a property of the scanning system itself, rather than a physiologic property of the brain, and can be observed with inert phantoms instead of human subjects (Smith et al., 1999; Zarahn et al., 1997). Other evidence has suggested drift effects may be influenced by spontaneous neuronal events and may be pixelwise dependent (Biswal et al., 1995; Hyde

et al., 2001). The slow drifts in the present study seem to arise primarily from the scanning system as we observed very similar levels of low-frequency noise in BOLD data at both 1.5 and 4 T. Since brain physiological noise has been reported to increase at higher field strength (Krueger et al., 2001), it would be reasonable to speculate that the drift effect would be more pronounced at 4 T if it is primarily of physiological origin. It is worth mentioning that the performance of our scanners is comparable with reported values indicated by published stability tests (Weisskoff, 1996). The absence of temporal autocorrelation in the ASL perfusion data can be largely attributed to the pairwise subtraction that generates perfusion images. To a first approximation, pairwise subtraction of adjacent points results in the first derivative of a time series  $f(t)$  and the Fourier transform of the first derivative is  $i\omega F(\omega)$  [where  $F(\omega)$  is the Fourier transform of  $f(t)$ ]. As demonstrated previously, the power distribution of the raw gradient-echo image series follows the function of  $1/\omega$  (Zarahn et al., 1997). Therefore, the magnitude of the Fourier transform of its derivative will be 1, and stable noise characteristic over the entire frequency spectrum is expected. This effect was demonstrated by simulation and experimental results from a previous study (Aguirre et al., 2002) as well as the current results.

Considering the time scale of the CBF hemodynamic function (Yang et al., 2000) as opposed to the applied sample rate of every 6 s, perfusion image series could conceivably demonstrate a certain degree of temporal autocorrelation even after the substantial autocorrelation in the raw EPI images is minimized by pairwise subtraction. The absence of this effect in our data may suggest that the level of spontaneous drift in CBF is lower than the fluctuation in blood oxygenation. This difference may occur because ASL contrast reflects a single physiological parameter (perfusion), whereas the BOLD signal is not only affected by physiological parameters such as CBF, blood volume, and oxygenation consumption (Kwong et al., 1992; Mandeville et al., 1999; Ogawa et al., 1993), but also susceptible to biophysical effects, including small changes in scanner conditions (Smith et al., 1999). Another explanation might be that the temporal autocorrelation in perfusion signal is too small to be detected in our experiments due to the relatively low SNR of ASL methods, which results in greater thermal and scanner noise compared to physiological noise in perfusion data. Additionally, other sources of “colored” noise such as motion and artifacts from imperfections of the radiofrequency pulses could contaminate the perfusion data, making it deviate from the rigorous “white noise” property. These tentative speculations await experimental verification.

Our results also demonstrate that perfusion data generated using surround subtraction deviate to a certain extent from a strictly even power distribution and have higher false-positive rates than the theoretically expected value. The surround subtraction approach was originally proposed to deal with the time lag of one TR between label and

control acquisitions as well as to dampen the high frequency fluctuation in signal through averaging the two surrounding acquisitions (Wong et al., 1997). However, surround averaging behaves just like temporal smoothing on the raw image series and induces more weighting on the lower frequency range of the power spectrum. The resultant power spectrum of the perfusion image series might no longer be flat, leading to false-positive rates inconsistent with theory. The results of the normalized SD measurements show surround subtraction produces the smoothest perfusion time series with the lowest temporal fluctuation level among all perfusion data, adding support to the above point. Sinc interpolation shifts the label or control image series by one TR through modulating the phase in the frequency domain and keeps the magnitude of the power spectrum of the raw image series unchanged. Based on these results, both simple and sinc subtractions, especially in combination with spatial smoothing, are recommended in the application of perfusion fMRI to produce acceptable statistical inferences. Sinc subtraction has the advantage of eliminating the effect of the time lag between control and label acquisitions. More importantly, sinc subtraction minimizes the presence of oxygenation effects in the perfusion signal, which may alter the shape of the response and reduce experimentally evoked variance (Aguirre et al., 2002).

The results of the temporal characteristic of spatial coherence in perfusion data demonstrated that measures of SC follow an even distribution across frequencies, in contrast to the SC in BOLD data that is greater at lower frequencies. This important feature renders spatial smoothing beneficial in preserving the intrinsic noise property of perfusion data, whereas BOLD data become more autocorrelated after spatial smoothing. In fact, our analyses demonstrated that spatial smoothing improves the false-positive rates in perfusion data to be closer to the tabular value, yielding more accurate statistical results assuming independence in observations. The existence of the spatial coherence in perfusion data was also proven by correlation analyses with the global signal, though the causes of the spatial coherence are not yet understood. The spatial pattern of the global signal and the mean correlation coefficients averaged across ROIs of gray and white matter and CSF did not suggest a tissue-specific mechanism. It is unclear whether the global signal in perfusion data results from the raw image series through subtraction, from the physiological noise of CBF itself, or possibly from both factors.

Another interesting finding in the present study is that spatial coherence in the perfusion fMRI data is greater at high field compared to low field, as demonstrated by the correlation analyses and the measures of map smoothness as the voxel size of FWHM. Incidentally, the concurrently derived BOLD contrast data also show a trend of increased spatial coherence with field strength. The reason for these phenomena is not well understood. We previously reported that the ASL signal increases with field strength and that physiological noise, including metabolic fluctuations, tissue

motion, and pulsation also increases at high magnetic field (Wang et al., 2002). Our observation that the 4.0-T perfusion data do not show significantly reduced level of normalized temporal SD compared to 1.5-T perfusion data is consistent with these previous findings. It is reasonable to speculate that the increased level of physiological noise at high field might result in greater spatial coherence in the image series since much of the physiological noise arises from global effects such as cardiac or respiratory pulsation (Jezzard, 1999). The absence of differences between brain tissue components in the correlation analysis with global signal indicates that the current perfusion method may be more sensitive to global sources of physiological noise than other tissue-specific noise sources. Previous studies on BOLD fMRI have demonstrated a global shift in the main field, primarily caused by respiration at high magnetic field (Hu and Kim, 1994; Pfeuffer et al., 2002), and tissue-specific noise was noted when the physiological noise induced by pulsation has been removed (Kruger and Glover, 2001). Whether a similar mechanism underlies the temporal noise in perfusion fMRI awaits further investigation.

It has been reported that the magnitude of brain physiological noise is proportional to the echo time (TE) and raw image intensity, producing the maximum noise magnitude at  $TE = T_2^*$  and the minimum at  $TE = 0$  (Hyde et al., 2001; Kruger and Glover, 2001). In the current experiments, a constant TE of 18 ms was used in the PASL sequence at both 1.5 and 4.0 T. This value is much closer to the  $T_2^*$  of brain tissue at 4.0 T (about 20–30 ms) than at 1.5 T (about 60–70 ms) and probably accounts for the increased physiological noise and greater spatial coherence observed in the perfusion and BOLD data acquired using the PASL sequence at high field as compared to low field. Six subjects in our experiments were also scanned using optimized BOLD sequence under no behavioral paradigm conditions at each field respectively, with TE of 28 ms at 4.0 T and 50 ms at 1.5 T. The spatial coherence in these optimized BOLD data sets measured as correlation coefficients with global signal do not show significant difference between 1.5- and 4.0-T data (data not shown). Thus, the trend of increased physiological noise and spatial coherence in perfusion data with field strength may be attributable to the use of the minimum TE regardless of field strength. It is still unclear whether differences in hardware performance at 1.5 and 4 T, such as the B1 field homogeneity, play a role in generating the more spatially coherent noise at high field, although the optimized BOLD data seem not to support such speculation. Currently, the problem of relatively high noise level at high field can be partly addressed by including the global signal as a covariate in the GLM, which can reduce the residual temporal fluctuation of the 4.0-T data to a level no greater than that at 1.5 T. However, the issue of whether to include a global signal covariate becomes more complicated in the presence of spatially extended, experimentally induced variance (Aguirre et al., 1997, 1998; Desjardins et al., 2001). In future applications of perfusion fMRI, acquisition methods

with extremely short TE like SPIRAL and half K-space EPI methods may be used with ASL to reduce noise and reduce sensitivity to static susceptibility effects, especially for high field studies.

In the present study, the BOLD signals were derived from the average of the label and control acquisitions of PASL scans. Simulation has demonstrated that this procedure should not change the noise properties of the BOLD signals if they were derived from either the control or label acquisitions alone. A preliminary analysis comparing BOLD signals from pairwise averaging and the control acquisitions on three subjects showed very similar results in power spectrum, spatial coherence, and temporal stability. The results reported above were based on a pulsed ASL technique. The even distribution of the power spectrum in perfusion data has also been demonstrated using a continuous ASL (CASL) method (Aguirre et al., 2002). However, noise properties of these two classes of ASL techniques may differ as CASL offers higher SNR and less pulsatility effect due to its relatively long width of labeling pulses (Wang et al., 2002). It is also possible that other PASL techniques such as QUIPSS would generate different results as compared to the present study, given different pulse sequence structure and varying off-resonance effects in these methods. The generalization of the current results for all perfusion fMRI methods therefore needs further investigations on various scanning systems using different pulse sequences and imaging parameters.

## Conclusions

The main findings of the present study are (1) perfusion fMRI time series based on ASL contrast do not have substantial temporal autocorrelation and are roughly independent in time. However, surround subtraction was found to produce a slight excess of false positives. (2) Spatial coherence in perfusion data is consistent across different frequencies. Thus, spatially smoothed perfusion data preserve the relatively even power distribution when analyzed using a GLM assuming independence of observations. (3) Spatial coherence of the ASL data was found to be greater at high magnetic field than low field and spatial smoothing plus including the global signal as a covariate in the GLM helped reduce the noise level in perfusion fMRI, especially at high magnetic field.

## Acknowledgments

This research was supported by NIH Grants HD39621 and DA015149 and NSF Grant BCS0224007. The authors are grateful to Kathy Tang, Marcie Rabin, and Anne Roc for their help with the experiments.

## References

- Aguirre, G.K., Detre, J.A., Zarahn, E., Alsop, D.C., 2002. Experimental design and the relative sensitivity of BOLD and perfusion fMRI. *Neuroimage* 15, 488–500.
- Aguirre, G.K., Zarahn, E., D'Esposito, M., 1997. Empirical analyses of BOLD fMRI statistics. II. Spatially smoothed data collected under null-hypothesis and experimental conditions. *Neuroimage* 5, 199–212.
- Aguirre, G.K., Zarahn, E., D'Esposito, M., 1998. The inferential impact of global signal covariates in functional neuroimaging analyses. *Neuroimage* 8, 302–306.
- Alsop, D.C., Detre, J.A., 1996. Reduced transit-time sensitivity in noninvasive magnetic resonance imaging of human cerebral blood flow. *J. Cereb. Blood Flow Metab.* 16, 1236–1249.
- Biswal, B., Yetkin, F.Z., Haughehton, V.M., Hyde, J.S., 1995. Functional connectivity in the motor cortex of resting human brain using echo-planar imaging. *Magn. Reson. Med.* 34, 537–541.
- Bottomley, P.A., Hardy, C.J., Argersinger, R.E., Allen-Moore, G., 1987. A review of 1H nuclear magnetic resonance relaxation in pathology: are T1 and T2 diagnostic? *Med. Phys.* 14, 1–37.
- Cho, Z.H., Ro, Y.M., Park, S.T., Chung, S.C., 1996. NMR functional imaging using a tailored RF gradient echo sequence: a true susceptibility measurement technique. *Magn. Reson. Med.* 35, 1–5.
- Constable, R.T., Spencer, D.D., 1999. Composite image formation in z-shimmed functional MR imaging. *Magn. Reson. Med.* 42, 110–117.
- Deichmann, R., Josephs, O., Hutton, C., Corfield, D.R., Turner, R., 2002. Compensation of susceptibility-induced BOLD sensitivity losses in echo-planar fMRI imaging. *Neuroimage* 15, 120–135.
- Desjardins, A.E., Kiehl, K.A., Liddle, P.F., 2001. Removal of confounding effects of global signal in functional MRI analyses. *Neuroimage* 13, 751–758.
- Detre, J.A., Alsop, D.C., 1999. Perfusion fMRI with arterial spin labeling (ASL). in: Moonen, C.T.W., Bandettini, P.A. (Eds.), *Functional MRI*. Springer-Verlag, Heidelberg, pp. 47–62.
- Detre, J.A., Wang, J., 2002. Technical aspects and utilities of fMRI using BOLD and ASL. *Clin. Neurophysiol.*, in press.
- Detre, J.A., Zhang, W., Roberts, D.A., Silva, A.C., Williams, D.S., Grandis, D.J., Koretsky, A.P., Leigh, J.S., 1994. Tissue specific perfusion imaging using arterial spin labeling. *NMR Biomed.* 7, 75–82.
- Duong, T.Q., Kim, D.K., Ugurbil, K., Kim, S.G., 2001. Localized cerebral blood flow response at submillimeter columnar resolution. *Proc. Natl. Acad. Sci. USA* 98, 10904–10909.
- Friston, K.J., Ashburner, J., Frith, C.D., Poline, J.B., Heather, J.D., 1995. Spatial registration and normalization of images. *Hum. Brain Mapp.* 3, 165–189.
- Friston, K.J., Jezzard, P., Turner, R., 1994. Analysis of functional MRI time-series. *Hum. Brain Mapp.* 1, 153–174.
- Friston, K.J., Josephs, O., Zarahn, E., Holmes, A.P., Rouquette, S., Poline, J., 2000. To smooth or not to smooth? *Neuroimage* 12, 196–208.
- Hu, X., Kim, S.G., 1994. Reduction of signal fluctuation in functional MRI using navigator echoes. *Magn. Reson. Med.* 31, 495–503.
- Hyde, J.S., Biswal, B.B., Jesmanowicz, A., 2001. High-resolution fMRI using multislice partial k-space GR-EPI with cubic voxels. *Magn. Reson. Med.* 46, 114–125.
- Jezzard, P., 1999. Physiological noise: strategies for correction, in: Moonen, C.T.W., Bandettini, P.A. (Eds.), *Functional MRI*. Springer-Verlag, Heidelberg, pp. 173–182.
- Kiebel, S.J., Poline, J.B., Friston, K.J., Holmes, A.P., Worsley, K.J., 1999. Robust smoothness estimation in statistical parametric maps using standardized residuals from the general linear model. *Neuroimage* 10, 756–766.
- Kim, S.G., 1995. Quantification of relative cerebral blood flow change by flow-sensitive alternating inversion recovery (FAIR) technique: application to functional mapping. *Magn. Reson. Med.* 34, 293–301.
- Krueger, G., Kastrup, A., Glover, G.H., 2001. Neuroimaging at 1.5T and 3.0T: comparison of oxygenation-sensitive magnetic resonance imaging. *Magn. Reson. Med.* 45, 595–604.
- Krueger, G., Glover, G.H., 2001. Physiological noise in oxygenation-sensitive magnetic resonance imaging. *Magn. Reson. Med.* 46, 631–637.
- Kwong, K.K., Belliveau, J.W., Chesler, D.A., Goldberg, I.E., Weisskoff, R.M., Poncelet, B.P., Kennedy, D.N., Hoppel, B.E., Cohen, M.S., Turner, R., 1992. Dynamic magnetic resonance imaging of human brain activity during primary sensory stimulation. *Proc. Natl. Acad. Sci. USA* 89, 5675–5679.
- Luh, W.M., Wong, E.C., Bandettini, P.A., Ward, B.D., Hyde, J.S., 2000. Comparison of simultaneously measured perfusion and BOLD signal increases during brain activation with T(1)-based tissue identification. *Magn. Reson. Med.* 44, 137–143.
- Mandeville, J.B., Marota, J.J., Ayata, C., Moskowitz, M.A., Weisskoff, R.M., Rosen, B.R., 1999. MRI measurement of the temporal evolution of relative CMRO(2) during rat forepaw stimulation. *Magn. Reson. Med.* 42, 944–951.
- Ogawa, S., Menon, R.S., Tank, D.W., Kim, S.G., Merkle, H., Ellerman, J.M., Ugurbil, K., 1993. Functional brain mapping by blood oxygenation level-dependent contrast magnetic resonance imaging. A comparison of signal characteristics with a biophysical model. *Biophys. J.* 64, 803–812.
- Ordidge, R.J., Wylezinska, M., Hugg, J.W., Biutterworth, E., Franconi, F., 1996. Frequency offset corrected inversion (FOCI) pulses for use in localized spectroscopy. *Magn. Reson. Med.* 36, 562–566.
- Pfeuffer, J., Van de Moortele, P.F., Ugurbil, K., Hu, X., Glover, G.H., 2002. Correction of physiologically induced global off-resonance effects in dynamic echo-planar and spiral functional imaging. *Magn. Reson. Med.* 47, 344–353.
- Raichle, M.E., Eichling, J.O., Straatmann, M.G., Welch, M.J., Larson, K.B., Ter-Pogossian, M.M., 1976. Blood-brain barrier permeability of 11C-labeled alcohols and 15O-labeled water. *Am. J. Physiol.* 230, 543–552.
- Smith, A.M., Lewis, B.K., Ruttimann, U.E., Ye, F.Q., Sinnwell, T.M., Yang, Y., Duyn, J.H., Frank, J.A., 1999. Investigation of low frequency drift in fMRI signal. *Neuroimage* 9, 526–533.
- Wang, J., Aguirre, G.K., Kimberg, D.Y., Roc, A.C., Li, L., Detre, J.A., 2003a. Arterial spin labeling perfusion fMRI with very low task frequency. *Magn. Reson. Med.* 49, 796–802.
- Wang, J., Alsop, D.C., Li, L., Listerud, J., Gonzalez-At, J.B., Schnall, M.D., Detre, J.A., 2002. Comparison of quantitative perfusion imaging using arterial spin labeling at 1.5 and 4 telsa. *Magn. Reson. Med.* 48, 242–254.
- Wang, J., Li, L., Roc, A.C., Alsop, D.C., Tang, K., Butler, N., Schnall, M.D., Detre, J.A., 2003b. Reduced susceptibility effect in perfusion fMRI using single-shot spin-echo EPI acquisitions. *Magn. Reson. Imag.*, in press.
- Weisskoff, R.M., 1996. Simple measurement of scanner stability for functional NMR imaging of activation in the brain. *Magn. Reson. Med.* 36, 643–645.
- Weisskoff, R.M., Baker, J., Belliveau, J.W., Davis, T.L., Kwong, K.K., Cohen, M.S., Rosen, B.R., 1993. Power spectrum analysis of functionally-weighted MR data: what's in the noise? *Proc. Inter. Soc. Magn. Reson. Med.* 1, 7.
- Wong, E.C., 1999. Potential and pitfalls of arterial spin labeling based perfusion imaging techniques for MRI, in: Moonen, C.T.W., Bandettini, P.A. (Eds.), *Functional MRI*, Springer-Verlag, Heidelberg, pp. 63–69.
- Wong, E.C., Buxton, R.B., Frank, L.R., 1997. Implementation of quantitative perfusion imaging techniques for functional brain mapping using pulsed arterial spin labeling. *NMR Biomed.* 10, 237–249.
- Wong, E.C., Buxton, R.B., Frank, L.R., 1998a. Quantitative imaging of perfusion using a single subtraction (QUIPSS and QUIPSS II). *Magn. Reson. Med.* 39, 702–708.

- Wong, E.C., Buxton, R.B., Frank, L.R., 1998b. A theoretical and experimental comparison of continuous and pulsed arterial spin labeling techniques for quantitative perfusion imaging. *Magn. Reson. Med.* 40, 348–355.
- Woolrich, M.W., Ripley, B.D., Brady, M., Smith, S.M., 2001. Temporal autocorrelation in univariate linear modeling of fMRI data. *Neuroimage* 14, 1370–1386.
- Worsley, K.J., Liao, C.H., Aston, J., Petre, V., Duncan, G.H., Morales, F., Evans, A.C., 2002. A general statistical analysis for fMRI data. *Neuroimage* 15, 1–15.
- Worsley, K.J., Marrett, S., Neelin, P., Vandal, A.C., Friston, K.J., Evans, A.C., 1996. A unified statistical approach for determining significant signals in images of cerebral activation. *Hum. Brain Mapp.* 4, 58–73.
- Yang, Y., Engelen, W., Pan, H., Xu, S., Silbersweig, D.A., Stern, E., 2000. A CBF-based event-related brain activation paradigm: characterization of impulse-response function and comparison to BOLD. *Neuroimage* 12, 287–297.
- Yang, Y., Frank, J.A., Hou, L., Ye, F.Q., McLaughlin, A.C., Duyn, J.H., 1998. Multislice imaging of quantitative cerebral perfusion with pulsed arterial spin labeling. *Magn. Reson. Med.* 39, 825–832.
- Yang, Y., Wen, H., Mattay, V.S., Balaban, R.S., Frank, J.A., Duyn, J.H., 1999. Comparison of 3D BOLD functional MRI with spiral acquisition at 1.5 and 4.0 T. *Neuroimage* 9, 446–451.
- Ye, F.Q., Mattay, V.S., Jezzard, P., Frank, J.A., Weinberger, D.R., McLaughlin, A.C., 1997. Correction for vascular artifacts in cerebral blood flow values measured by using arterial spin tagging techniques. *Magn. Reson. Med.* 37, 226–235.
- Zarahn, E., Aguirre, G.K., D'Esposito, M., 1997. Empirical analyses of BOLD fMRI statistics. I. Spatially unsmoothed data collected under null-hypothesis conditions. *Neuroimage* 5, 179–197.